Article published online: 2023-11-22

Effects of 3D Airway Geometry on the Airflow of Adults with Cleft Lip and Palate and Obstructive Sleep Apnea: A Functional Imaging Study

Leticia Dominguez Campos[1] Inge Elly Kiemle Trindade[1,2,3] Sergio Henrique Kiemle Trindade[1,4] Luiz André Freire Pimenta[3] Julia Kimbell[5] Amelia Drake[5] Maria Noel Marzano-Rodrigues[1] Ivy Kiemle Trindade-Suedam[1,2,3]

[1] Laboratory of Physiology, Hospital de Reabilitação de Anomalias Craniofaciais, Universidade de São Paulo, Bauru, SP, Brazil
[2] School of Dentistry, University of North Carolina at Chapel Hill, Chapel Hill, NC, United States of America
[3] Department of Biological Sciences, School of Dentistry, Universidade de São Paulo, Bauru, SP, Brazil
[4] Department of Pediatric Dentistry, Orthodontics and Public Health, School of Medicine, Universidade de São Paulo, Bauru, SP, Brazil

Address for correspondence Ivy Kiemle Trindade-Suedam, Laboratório de Fisiologia, Hospital de Reabilitação de Anomalias Craniofaciais, Universidade de São Paulo, Bauru, SP, Brazil (e-mail: ivytrin@usp.br).

[5] School of Medicine, University of North Carolina at Chapel Hill, Chapel Hill, NC, United States of America

Sleep Sci 2023;16(4):e430–e438.

Abstract

Objective Individuals with cleft lip and palate (CLP) are at a high risk of developing obstructive sleep apnea (OSA). Hypothetically, the severity of OSA might be associated with the morphology of the upper airway (UAW) and the characteristics of the airflow. Thus, the present study aimed to assess and compare, in adults with CLP and skeletal class-III discrepancy, with or without OSA, simulations of airflow resistance and pressure according to the geometrical characteristics of the UAW and cephalometric parameters.

Materials and Methods According to the results of type-I polysomnography tests, the sample ($n = 21$) was allocated in 2 groups: 1) without OSA (N-OSA; $n = 6$); and 2) with OSA (OSA; $n = 15$). Cephalometric measurements were performed on the cone-beam computed tomography (CBCT) scans of the groups. After three-dimensional (3D) reconstructions, the volume (V) and minimal cross-sectional area (mCSA) of the UAW were generated. Computational fluid dynamics (CFD) simulations were used to assess key airflow characteristics. The results were presented at a significance level of 5%.

Results The UAW pressure values and airway resistance did not differ between the groups, but there was a tendency for more negative pressures (26%) and greater resistance (19%) in the OSA group. Volume and mCSA showed a moderate negative correlation with resistance and pressure. The more inferior the hyoid bone, the more negative the pressures generated on the pharyngeal walls.

Conclusion The position of the hyoid bone and the geometry of the UAW (V and mCSA) exerted effects on the airway-airflow resistance and pressure. However, key airflow characteristics did not differ among subjects with CLP, were they affected or not by OSA.

Keywords
- congenital, hereditary, and neonatal diseases and abnormalities
- diagnostic imaging
- sleep apnea, obstructive

received
June 25, 2022
accepted
February 9, 2023

DOI https://doi.org/10.1055/s-0043-1776868.
ISSN 1984-0659.

Thieme Revinter Publicações Ltda., Rua do Matoso 170, Rio de Janeiro, RJ, CEP 20270-135, Brazil

Introduction

Obstructive sleep apnea (OSA) is characterized by impaired normal ventilation during sleep due to narrowing of the upper airway' (UAW). This sleep-breathing disease causes significant morbidity if not treated.[1] Some patient populations are at increased risk of developing OSA, including those with cleft lip and palate (CLP),[1–4] which is the most prevalent congenital craniofacial malformation, occurring with a reported frequency that ranges from 0.18 to 4.04/1,000 neonates.[5,6]

The morphological craniofacial characteristics in CLP individuals can produce a decrease in airway patency, predisposing to OSA.[1] The anatomical narrowing can occur due to a reduced nasal cavity cross-sectional area (CSA) at the cleft side,[7] reduced pharyngeal volume,[3,8] and a more inferiorly positioned hyoid bone[9] or unfavorable maxillomandibular relationship.[10]

Since the last decade, computational fluid dynamics (CFD) has been validated as a reliable tool to study fluid aspects and fluid-structure interactions. In the biomedical field, CFD gained a great deal of relevance in the assessment of the airflow-airway interplay in obstructive airway diseases.[11–15] It has been demonstrated through CFD simulations that high variability in airway resistance and pressure can be associated with structure stenosis and a higher predisposition to develop sleep-breathing diseases.[13,16] However, CFD techniques have not been fully used for the evaluation of OSA induced by airway obstructions in the CLP population.

We considered the hypothesis that in CLP adults with class-III malocclusion and OSA, the impaired maxillomandibular relationship and reduced airway dimensions determine altered airflow parameters. Thus, the present study was developed to investigate and quantify the correlations among airway 3D geometry, and cephalometric, polysomnographic (PSG), and airflow characteristics in this particular sample.

Materials and Methods

Ethical Considerations

The present study was approved by the institutional review board (Process number omitted for peer review). The study protocol was in accordance with the guidelines of the Health Insurance Portability and Accountability Act of 1996 (HIPAA) and the 1964 Declaration of Helsinki, or comparable ethical standards. All of the participants signed an informed consent form agreeing to participate in the study.[3]

Health and Safety

All mandatory laboratory health and safety procedures have been complied with in the course of the present study.

Study Subjects and Groups

The subjects assessed in the present study also comprised the groups on the study by Campos et al.[3] Therefore, the criteria for participant selection, sample characterization, and protocol for cone-beam computed tomography (CBCT) acquisition can be fully obtained in the aforementioned article.

Briefly, the study sample was prospectively selected among adults with repaired CLP and class-III malocclusion with scheduled orthognathic surgery. After excluding individuals with conditions involved in airway obstruction and reduced pharyngeal dimensions other than CLP, such as hypertrophic tonsils, the presence of pharyngeal flap, or obesity, 21 subjects were enrolled. They were submitted to CBCT scans that required for preoperative purposes, using the i-CAT Next Generation Cone Beam (Imaging Sciences International, Hatfield, PA, United States; field of view of 16 cm x 13 cm; exposure time of 26.9 seconds; 120 kV; 37 mA; and resolution of 0.25 voxels).

As mentioned in the study by Campos et al.,[3] the sample was divided into two groups according to PSG results: 1) obstructive sleep apnea (OSA; $n = 6$; 5 male patients; apnea-hypopnea index [AHI]: $\geq$ 5 events/hour; mean age: 24 ± 3 years, and mean neck circumference: 37 ± 3 cm); and 2) non-OSA (N-OSA; $n = 15$; 10 male patients; AHI < 5 events/hour; mean age: 25 ± 3 years; mean neck circumference: 39 ± 2 cm).[1] No significant differences were observed between the groups regarding age and neck circumference.

Upper Airway Reconstruction

Digital Imaging and Communications in Medicine (DICOM) files from the CBCT scans were imported into the Mimics Research software, version 17.0 (Materialise, Leuven, Belgium). The selected threshold range was between -1024 and -400. A combination of manual slice and 3D editing was performed to obtain the UAW segmentation, including the nasal cavity and pharynx. Lastly, from the mask involving the final region of interest, the 3D models were generated. In the present study, 3D images were used for CFD simulations.

Computational Fluid Dynamics Simulations

Geometry and Mesh Generation

The geometry was created from stereolithographic (STL) files of the 3D reconstructions from the airway of each subject and imported from the Mimics Research software (Materialise) to the ICEM-CFD (ANSYS, Inc., Canonsburg, PA, United States) meshing software. The surfaces of the airway walls, the inlet (nostrils), and outlet (the most inferior portion of the pharynx on the CBCT scan), were created separately.[11,13,14] Hybrid meshes with tetrahedron and three-layered prism walls were created, assuming the intrinsic complexity of the UAW morphology. The mesh sizing was of 4×10^6 elements.[11,13,14,17] To minimize distortion effects, mesh quality was assessed to ensure that the aspect ratio ($\mathrm{AR} = \frac{long\ edge\ lenght}{short\ edge\ length}$) of the elements was of at least 0.3.[17]

Airflow Simulations

Using the Fluent solver (ANSYS, Inc.), version 14, laminar inspiratory airflow simulations were conducted under physiologic pressure-driven conditions.[11,13] The resting minute volumes were estimated based on body weight using allometric scaling.[11] Male and female data were calculated through different equations respectively:

$\dot{V}_E = (1.36 \pm 0.10)M^{0.44\pm0.02}$; $r = 0.095$; and
$\dot{V}_E = (1.89 \pm 0.40)M^{0.32\pm0.06}$; $r = 0.897$,

in which $\dot{V}_E$ is the minute volume in liters per minute, M is body mass in kilograms, and r is the correlation coefficient.[11] The steady-state inspiratory airflow rates were computed as two times the minute volume, assuming that inspiration and expiration had the same duration.[11]

The differential equations were solved through the finite volume method.[11,13] The mathematical equations for conservation of mass and momentum were represented respectively by:

$$\nabla.u=0; \text{ and}$$
$$p\frac{\partial u}{\partial t} + p\,(u.\nabla) = -\nabla p + \mu^2\, u,$$

in which $u = u$ (x, y, x, t) is the velocity vector, t is time, $p = 1.204 kg/m^3$ is the fluid density, p is pressure, and $\mu = 1.825^{-5}$ kg/ms is the dynamic viscosity.[11,13,18]

The selected boundary conditions for the airflow simulations were: 1) a pressure-inlet condition at the nostrils with gauge 0 Pascal (Pa); 2) stationary right and left nasal cavity and pharynx walls, with air velocity set to 0 at the air-wall interface; 3) an outlet condition with a negative pressure (-Pa) calculated for each patient, according to the previously estimated steady-state inhalation rate.

CFD Variables

Several CFD variables that can be correlated with UAW patency were investigated: 1) mean and maximum pressure in the wall of the total UAW, nasal cavity, pharynx and its segments; 2) mean and maximum pressure in the minimal CSA (mCSA) of the UAW; 3) pressure drop from the inlet to the outlet on the total UAW and on UAW segments; 4) resistance from the inlet to the outlet; and 5) pharyngeal resistance at its segments (nasopharynx, oropharynx, and hypopharynx).

The total airway resistance from the inlet to the outlet was computed as the pressure drop (ΔP) in -Pa divided by the flow rate (Q) in millimeters per second (mL/s). The local resistance in the pharynx segments was calculated by dividing the pressure at each area (p) by the volumetric flow rate passing through that cross-sectional segment (q).[13,16] The mathematical equations for pressure drop, total, and segment resistance were represented respectively by:

$$\Delta P = P_1 - P_2;$$
$$R_{TOTAL} = \frac{\Delta P}{Q}; \text{ and}$$
$$R_{SEGMENT} = \frac{p}{q}.$$

Cephalometric Analysis

A cephalometric analysis was performed to assess possible differences in horizontal skeletal patterns (the angle between the sella/nasion plane and the nasion/A plane [SNA], the angle between the sella/nasion plane and nasion/B plane [SNB], and the difference between the SNA and SNB [ANB]) and vertical growth patterns (sella/nasion to mandibular plane angle, SN-MP) between groups. Cephalometric parameters related to OSA occurrence, which assess the horizontal and vertical position of the hyoid bone related to several craniofacial landmarks (pharyngeal length, the distance from the mandibular plane to the hyoid bone [MP-H], the distance between the gonion [Go] and H [Go-H], the distance between the sella and H [S-H], the angle between the gnathion [Gn], Go, and H [GoGn-H], and the nasion-sella-hyoid [N-S-H] angle), were also evaluated and are described in ►**Table 1**.[19,20]

Table 1 Definitions of the cephalometric measurements at the sagittal aspect.

Variable	Measurements
Horizontal maxillomandibular discrepancy	
● SNA (°)	Angle subtended from the sella (S) by means of the nasion (N) to maxillary point A.
● SNB (°)	Angle subtended from S by means of N to mandibular point B.
● ANB (°)	The difference between the SNA and SNB.
Facial vertical pattern	
● SN-MP (°)	Angle between anterior cranial base (S-N) and the mandibular plane (MP).
Measures related to OSA (vertical and horizontal hyoid position related to craniofacial landmarks)	
● Pharynx length (mm)	Distance between ANS and H.
● MP-H (mm)	Distance between MP and the hyoid (H) bone.
● Go-H (mm)	Distance between the gonion (Go) and H.
● S-H (mm)	Distance between S and H.
● GoGn-H (°)	Angle between Go, gnathion (Gn), and H.
● N-S-H (°)	Angle subtended from N by means of S to H.

Abbreviation: OSA, obstructive sleep apnea.

The DICOM files were imported into the Dolphin Imaging software, version 11.7 Premium (Patterson Dental Supply, Inc., Saint Paul, MN, United States), for the cephalometric analysis. For the assessment, lateral cephalograms from 3D images were created out of the sagittal plane. The standardization of the head position was based on the axial (line passing through the lowest points of the right and left mastoid processes), coronal (Frankfort horizontal), and sagittal (line passing through the tip of the nasal bone and the most inferior point of the foramen magnum) planes.[21]

As mentioned by Trindade-Suedam et al.[8], the mean normative value of the SNA was of to $82 \pm 2°$, which means that values $< 80°$ represent maxillary retrusion, and values $> 84°$, maxillary protrusion. For the SNB, the mean normative value was of $80 \pm 2°$. Values $< 78°$ represent a retruded mandible, and $> 82°$, protruded mandible. And the mean normative value of the ANB was of $2 \pm 2°$. Negative values corresponded to class-III maxillomandibular discrepancy.

The same trained and blinded examiner assessed the cephalometric parameters twice, with an interval of 15 days between measurements. A second trained and blinded examiner evaluated 50% of the sample. High intra-examiner (0.96 to 0.99) and interexaminer (0.91 to 0.99) agreements were verified using the intraclass correlation coefficient (ICC).[3]

Statistical Analysis

Descriptive data are presented as mean and standard deviation (SD) values. The Student *t*-test and the Mann-Whitney test were used to compare the variables with normal and nonnormal distribution in the OSA and N-OSA groups respectively. Correlations among quantitative variables (CFD parameters and cephalometric measurements) were assessed using the Pearson correlation coefficient.

The strength of the associations between variables demonstrated through the Pearson and the Spearman tests was interpreted as: weak (r =0.30–0.49), moderate ($r = 0.50$–0.69), and strong ($r = 0.70$–1.00) correlations. The significance level was set at 0.05, and the IBM SPSS Statistics for Windows software, version 21.0 (IBM Corp., Armonk, NY, United States), was used for the statistical analysis.

Results

Inspiratory Pressure on the Airway Walls

The results of pressure obtained by means of CFD simulations are presented in ►**Table 2**. The mean (*P*mean) and maximum (*P*max) values for the wall pressure were assessed in the total UAW and its anatomical subdivisions (nasal cavity, pharynx, and pharyngeal segments) to estimate collapsibility. The pressure was also measured in the mCSA (*P*mCSA) of the pharynx of each subject. We observed that, from the inlet to the outlet (from the nasal cavity until the hypopharynx), the wall pressures became progressively negative (-Pa) on both groups. Although pressures were more negative in the OSA group (26% greater for the total airway) than in the N-OSA group, these differences were not statistically significant ($p > 0.05$). ►**Figure 1** and ►**Figure 2** show the qualitative results of the CFD simulations.

Resistance of the Airway to Airflow

The resistance of the total airway and its segments to inspiratory airflow did not differ between groups, despite the greater values among OSA subjects (19% greater for the

Table 2 Mean, minimum, and maximum absolute values of pressure (*P*) obtained from computational fluid dynamics simulations in the patients without (N-OSA) and with obstructive sleep apnea (OSA) (sample size = 21).

Airway segment *P* (-Pa)	N-OSA ($n = 15$)		OSA ($n = 6$)		Statistical significance* ($p \leq 0.05$)
	Mean ± SD	Min-max.	Mean ± SD	Min.-max.	
Airway *P*mean	**19 ± 11**	4–41	**22 ± 9**	12–35	0.287
Airway *P*max	**46 ± 28**	9–104	**50 ± 26**	25–89	0.369
Nasal *P*mean	**15 ± 9**	3–32	**18 ± 8**	10–31	0.450
Nasal *P*max	**34 ± 25**	9–89	**41 ± 22**	17–76	0.438
Pharynx *P*mean	**25 ± 14**	7–53	**30 ± 12**	16–46	0.480
Pharynx *P*max	**40 ± 25**	8–104	**46 ± 25**	24–89	0.278
Nasopharynx *P*mean	**23 ± 14**	7–48	**26 ± 10**	15–38	0.578
Nasopharynx *P*max	**27 ± 17**	8–59	**33 ± 13**	17–46	0.255
Oropharynx *P*mean	**26 ± 14**	7–55	**31 ± 13**	16–48	0.389
Oropharynx *P*max	**31 ± 15**	7–64	**37 ± 17**	18–60	0.204
Hypopharynx *P*mean	**31 ± 17**	7–67	**39 ± 15**	19–57	0.499
Hypopharynx *P*max	**39 ± 24**	8–104	**51 ± 24**	25–89	0.249
mCSA *P*mean	**30 ± 18**	7–67	**38 ± 12**	20–53	0.585
mCSA *P*max	**33 ± 23**	7–91	**41 ± 12**	23–57	0.526

Abbreviations: Max., maximum; mCSA, minimal cross-sectional area; Min., minimum; SD, standard deviation.
Notes: *$p \leq 0.05$; the Student *t*-test (two-tailed) was used to compare the means of the two groups.

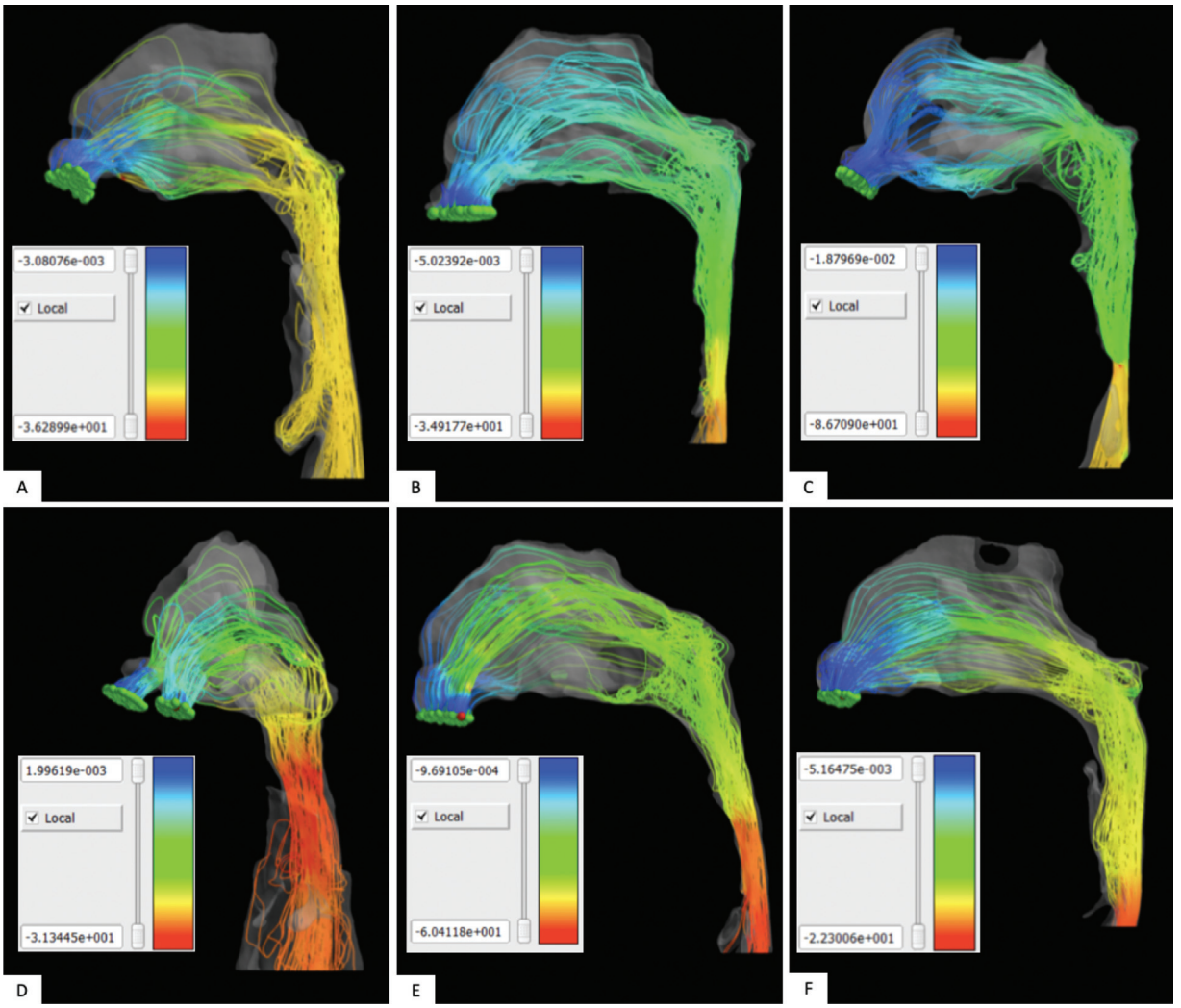

Fig. 1

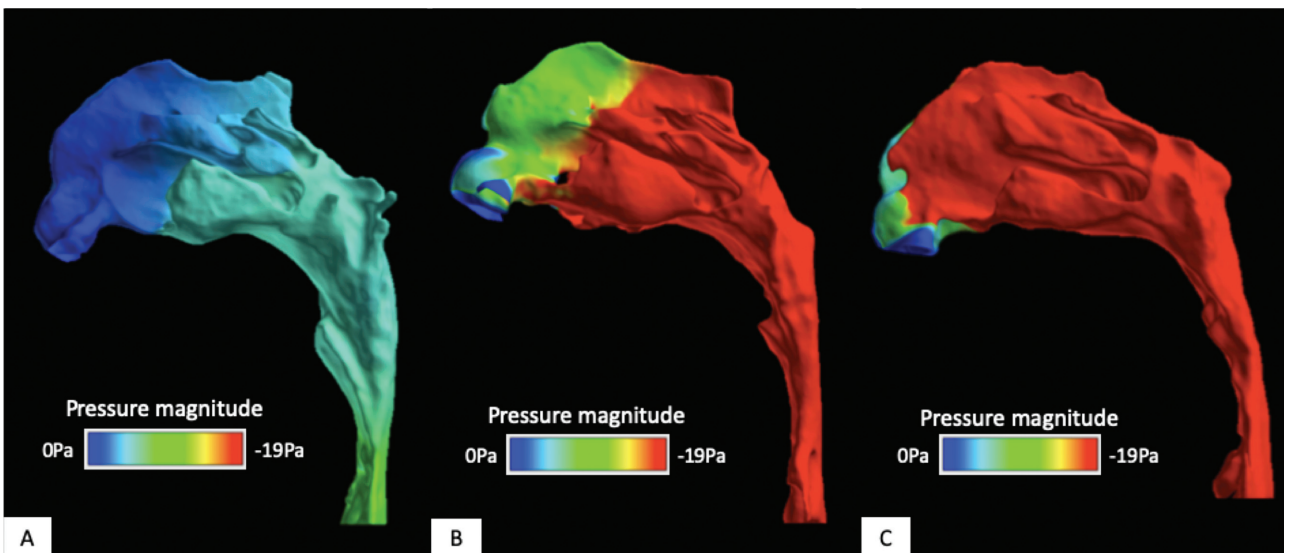

Fig. 2

Table 3 Mean, minimum, and maximum values of airway resistance (*R*) obtained from computational fluid dynamics analysis, in patients without (N-OSA) and with obstructive sleep apnea (OSA) (sample size = 21).

Airway segment *R* (Pa.s/mL)	N-OSA ($n = 15$)		OSA ($n = 6$)		**Statistical significance***
	Mean ± SD	Min-max	Mean ± SD	Min.-max.	
Airway	**0.111 ± 0.052**	0.030–0.218	**0.133 ± 0.043**	0.086–0.188	0.311
Nasal	**0.080 ± 0.043**	0.028–0.170	**0.095 ± 0.023**	0.064–0.124	0.218
Pharynx	**0.031 ± 0.032**	0.001–0.119	**0.039 ± 0.023**	0.015–0.077	0.359
Nasopharynx	**0.003 ± 0.004**	0.000–0.014	**0.010 ± 0.010**	0.000–0.025	0.091
Oropharynx	**0.111 ± 0.052**	0.030–0.218	**0.133 ± 0.043**	0.086–0.188	0.498
Hypopharynx	**0.080 ± 0.043**	0.028–0.170	**0.095 ± 0.023**	0.064–0.124	0.622

Abbreviations: Max., maximum; Min., minimum; SD, standard deviation.
Notes: *$p \leq 0.05$; the Student *t*-test (two-tailed) was used to compare the means of the two groups.

total airway; $p > 0.05$). Furthermore, both groups presented greater resistance values in the nasal cavity than in the pharynx ($p \leq 0.05$) (►**Table 3**).

Cephalometric Outcomes

No differences were observed between the N-OSA ($n = 15$) and OSA ($n = 6$) groups, regarding all cephalometric variables assessed, as seen on ►**Table 4** ($p > 0.05$). More specifically, class-III skeletal discrepancy was observed in 100% of the subjects assessed, and it was mainly related with isolated maxillary retrusion or with maxillary + mandibular retrusion, on both groups. Likewise, no differences in facial vertical pattern (SN-MP) were observed between groups. The cephalometric parameters related to OSA occurrence (MP-H, Go-H, S-H, GoGn-H, and SNH) did not differ at a statistically significant level ($p > 0.05$) between N-OSA and OSA groups.

Correlation Between Variables

Moderate negative correlations were found for the *P*max (total airway $r = -0.510$; pharynx $r = -0.543$; oropharynx $r = -0.503$; and hypopharynx $r = -0.560$) versus the S-H, for resistance (total airway $r = -0.544$; nasal cavity $r = -0.640$; and oropharynx $r = -0.557$) versus airway volume, and for resistance (pharynx $r = -0.684$; and oropharynx $r = -0.686$) versus. the mCSA. Moderate positive correlations were found for nasal cavity volume versus mean inspiratory pressure ($r = 0.532$) and for mCSA versus *P*max (pharynx $r = 0.519$; and hypopharynx $r = 0.550$). The area and volumetric data were obtained from Campos et al.[3]

Discussion

A considerable number of adults with repaired CLP present with OSA and related symptoms. Besides the classic risk factors for OSA, like obesity and advanced age, congenital UAW abnormalities and the presence of a pharyngeal flap for the correction of velopharyngeal insufficiency are the main predisposing factors for the sleep breathing disorders of this population.[3,22] However, there is still no complete understanding of the etiopathogenesis of OSA in CLP.

Table 4 Mean, minimum, and maximum cephalometric values in patients without (N-OSA) and with obstructive sleep apnea (OSA) (sample size = 21).

Variable*	N-OSA ($n = 15$)		OSA ($n = 6$)		Statistical significance**
	Mean ± SD	Min.-max.	*X* Mean ± SD	Min.-max.	
SNA (°)	**75 ± 4**	68–83	**75 ± 4**	68–79	0.276
SNB (°)	**80 ± 4**	71–88	**78 ± 5**	70–84	0.166
ANB (°)	**-6 ± 4**	-1–15	**-3 ± 3**	- 0.4–6	0.103
SN-MP (°)	**35 ± 5**	24–46	**39 ± 6**	29–47	0.070
Pharynx length (mm)	**70 ± 9**	55–86	**71 ± 7**	65–79	0.798
MP-H (mm)	**16 ± 6**	7–26	**17 ± 6**	7–22	0.860
Go-H (mm)	**37 ± 7**	27–51	**37 ± 9**	23–48	0.581
S-H (mm)	**108 ± 10**	92–124	**110 ± 10**	100–125	0.785
GoGn-H (°)	**27 ± 10**	10–48	**27 ± 10**	12–41	0.355
N-S-H (°)	**89 ± 4**	81–97	**90 ± 5**	85–98	0.455

Notes: *For the explanation of the acronyms in the Variable column, see table 1. **$p \leq 0.05$; the Student *t*-test (two-tailed) was used to compare the means of the two groups.

Earlier, Trindade-Suedam et al.[8] demonstrated that adults with CLP and skeletal class-III discrepancy due to maxillary retrusion have significantly reduced pharyngeal volume and mCSA than individuals without CLP and with the same type of maxillomandibular discrepancy. After that, Campos et al.[3] observed that young adults with CLP and class-III malocclusion presented a clinically significant prevalence of OSA (29%), greater than that observed among the general Brazilian population of the same age range, of $\sim$ 7%.[23] Next, they[3] presented pioneering and promising results concerning the association of airway dimensions and OSA occurrence in the CLP population by showing that OSA occurrence was also associated with impaired airway volume, especially at the oropharyngeal level. Previous studies demonstrated that regardless of the body mass index (BMI), the severity of OSA was associated with mCSA of the oropharynx in adults without CLP.[24]

On the other hand, despite the findings by Campos et al.[3] strongly suggesting an association between airway morphology and impaired function, CFD simulations seemed to be required to verify the pattern of airway-airflow interactions. To accomplishing this, CFD simulations were performed in the present study in the same N-OSA and OSA groups previously studied by Campos et al.[3] To the best of our knowledge, correlations concerning OSA, airway geometry, cephalometric measurements, and CFD parameters in a sample with these particular characteristics were investigated for the first time in the present study. However, a parsimonious interpretation of these results is mandatory due to the reduced sample size, which may not represent the overall CLP population.

The difficulties to gather a large sample occurred for the following main reasons: 1) low level of compliance with the PSG examination; 2) difficulties in reconciling the PSG examination in the immediate preoperative period for orthognathic surgery; and 3) ethical restrictions on the use of ionizing radiation for research purposes only. An additional limitation is that the study did not include a control group of CLP adults without maxillomandibular discrepancy. Given the high prevalence of class-III in this population, as proved after the screening of hundreds of radiographic exams, gathering subjects for this other group was unfeasible.

In the present study, the hypothesis that respiratory events are associated with altered airflow parameters could not be confirmed. The CFD parameters, such as inspiratory pressure, were similar on the airway of N-OSA and OSA subjects. However, there was a tendency for more negative pressures in the OSA group, with a rate 26% greater than that of the N-OSA group. Similarly, no differences in resistance values were observed between the groups, even though resistance in the airways of OSA subjects was 19% greater than in the N-OSA group, as expected.

In other words, although we could not find statistically significant differences between groups, from a clinical point of view, our results show that patients diagnosed with OSA, even those with mild or moderate apnea, present a less patent UAW, that is, an airway more resistant to airflow. Consequently, they develop more negative pressures on the airway during inspiration.

The lack of correlation of these variables in the CLP subjects evaluated can be related to the small sample size, as previously mentioned, and to the occurrence of mild OSA instead of severe disease, indicated by AHI magnitude. As seen in non-CLP adults with OSA, an increase in wall shear stress, pressure drop, and velocity magnitude related exclusively with higher AHI.[25,26] Moreover, we observed that the adjusted pressure coefficient (PC) strongly correlated with the AHI ($r = 0.91$).

It is worth noting that relevant results were found concerning the association between the geometry of the UAW and airflow dynamics parameters. The pharyngeal mCSA showed a positive correlation with pharynx and hypopharynx *P*max: the smaller the areas, the more negative the pressures observed on the airway.

Moreover, the mCSA of the pharynx showed a negative correlation with the total pharyngeal resistance and the resistance at the oropharyngeal segment. Besides, total airway volume and resistance showed a negative correlation: the smaller the airway volumes and areas, the greater the airway resistance and the pressures generated in response to airflow. Finally, a moderate negative correlation was also observed between the airway *P*max and the S-H: the more inferior the hyoid bone, the more negative the pressures generated on the pharyngeal walls.

The impact of morphology over airflow behavior becomes evident when the concepts of pressure and resistance are reviewed. Pressure can be considered the amount of force that the airflow exerts on the airway walls. In contrast, resistance is the opposition to airflow caused by friction forces, represented by the ratio of a given pressure to airflow rate.[27] Therefore, the greater negative *P*max within the pharynx and hypopharynx suggest an increased risk of collapsibility of the airway (especially the mCSA) in CLP adults. It can also be inferred from the correlation between the mCSA of the pharynx and the increased resistance to airflow in the pharyngeal airway that a reduced diameter of the airway would play a role in the pathogenesis of OSA. Once again, despite no significant differences being observed between the N-OSA and OSA groups for both CFD parameters, the mean pressure values were more negative, and resistance was greater, among subjects with sleep-disordered breathing.

The influence of mCSA over pressure and resistance was, at least partially, illustrated by Poiseuille law and Bernoulli flow obstruction theory, as demonstrated in previous studies.[11,13,19] According to the law of Poiseuille, as stated in the equation $Q = \frac{\pi p r^4}{8\eta l}$ (in which Q is flow rate, p is pressure, r is radius, η is viscosity, and *l* is length), the airflow is inversely proportional to the fourth power of the internal diameter of the structure.[28] Considering the theory of Bernoulli, represented by the power law $R = aA^b$ (in which *a* is a constant and b is an exponent ranging from -0.85 and -1.07), the relative reduction in airflow is directly proportional to the relative reduction in airway CSA, namely $\left(\frac{Q_{OBTRUCTION}}{Q_{HEALTHY}} = k\frac{A_{OBSTRUCTION}}{A_{HEALTHY}}\right)$ (in which *k* is 0.25 ± 0.15).[13]

In the present study, all the CBCT examinations were performed with the patient awake, seated, and with the

head in a natural position, as recommended by the scanner manufacturer. Therefore, the geometrical characteristics of the airway are representative of the wakefulness state, which can be a limitation, considering that one of the objectives was to verify the correlation involving airway geometry and airflow behavior with respiratory events during sleep. As known, sleep induces a decrease in compensatory tonic input to motor neurons of dilatator muscles in the pharynx, which can be more significant in an anatomically impaired-UAW, as presented by CLP subjects.[29] Also, during sleep, the positions of the tongue, jaw, and hyoid vary according to the head posture (supine, prone, lateral recumbent, neutral, extended, flexed), which certainly impacts the UAW dimensions and its response to airflow.[30] Additionally, the compliance of the airway, which can vary in each subject during inspiratory-expiratory events, would influence our results.[25]

The CFD method is a powerful tool to analyze and solve fluid-flow problems. It is widely applicable for biomedical research, providing a better understanding of airway mechanisms during breathing in physiological or pathological conditions. Moreover, it becomes a compelling resource for surgery planning, providing useful preliminary information on treatment outcomes.[15] We adopted the commercial software Fluent platform (ANSYS Inc.) since it can handle the complex geometry of the UAW model.[14,17] However, several challenges can arise when evaluating airflow aspects through CFD during the preprocessing, solver, and postprocessing stages.[15]

To perform CFD simulations on the most accurate model, we reconstructed the UAW according to the actual dimensions and anatomical characteristics, avoiding simplifying the structure. The geometry model was created on CBCT images because they have an optimal contrast regarding airway space, soft tissues, and bones, and a relatively low radiation dose.[3] Considering that the paranasal sinuses have a minimal effect on the UAW airflow patterns, these structures were not included in the analysis.[11]

The tetrahedral-elements mesh method was chosen since it is considered the most adequate for the generation of grids in complex geometries, as is the case of the UAW. Moreover, the transition is less problematic than for the hexahedral-elements mesh, helping in the convergence of iterative methods to solve differential equations. Additionally, the mesh refinement can be performed locally. It could be argued that no sensitivity analysis was conducted to determine the optimal number and type of elements since this step is crucial to provide accurate numerical solutions for studies involving CFD. However, the mesh characteristics were based on the study for grid sensitivity of Frank-Ito et al.,[17] a popular technique to ensure the accuracy and consistency of the CFD model.[15]

In the present study, the cyclic nature of airflow and turbulence were not considered, and the airflow simulations were limited to steady-state laminar conditions.[11] As considered by Subramaniam et al.[31] and Kimbell et al.,[32] turbulence modeling is not necessary to obtain valuable results for resting breathing, as herein considered. However, despite nasal and pharyngeal airflow being described as laminar for resting breathing in individuals without craniofacial anomalies,[32] it is possible in the nostril affected by the fissure, the airflow assumes a more turbulent characteristic. Considering that a turbulent flow can show relatively larger pressure and velocity than laminar flow, complementary studies should be performed in CLP populations shortly.

In conclusion, the present study provided new information on the association of cephalometric parameters, UAW geometry, OSA, and airflow characteristics. Considering the studied sample and obtained data, we assume that the geometry of the UAW indeed exerts effects on the airway-airflow resistance and pressure, especially at the level of the nasal cavity. However, key airflow characteristics did not differ between subjects with CLP and skeletal class-III pattern affected or not by OSA. Future studies with larger samples are warranted to overcome the current limitations responsible for the inconclusive results concerning OSA occurrence and alteration in airflow characteristics. The potential of CFD to elucidate the effect of airway morphology, especially at sites more prone to collapse, on airflow resistance and pressure, makes it a compelling tool to better comprehend OSA in the CLP population.

Funding
The authors declare that the present work was supported by the Conselho Nacional de Desenvolvimento Científico e Tecnológico (CNPq).

Conflict of Interests
The authors have no conflict of interests to declare.

References

1 Kapur VK, Auckley DH, Chowdhuri S, et al. Clinical Practice Guideline for Diagnostic Testing for Adult Obstructive Sleep Apnea: An American Academy of Sleep Medicine Clinical Practice Guideline. J Clin Sleep Med 2017;13(03):479–504
2 Fernandes MBL, Salgueiro AGNS, Bighetti EJB, Trindade-Suedam IK, Trindade IEK. Symptoms of Obstructive sleep apnea, nasal obstruction, and enuresis in children with nonsyndromic cleft lip and palate: a prevalence study. Cleft Palate Craniofac J 2019;56 (03):307–313
3 Campos LD, Trindade I, Yatabe M, et al. Reduced pharyngeal dimensions and obstructive sleep apnea in adults with cleft lip/palate and Class III malocclusion. Cranio 2019;•••:1–7
4 Görücü-Coşkuner H, Saglam-Aydinatay B, Aksu M, Ozgur FF, Taner T. Comparison of positive screening for obstructive sleep apnea in patients with and without cleft lip and palate. Cleft Palate Craniofac J 2020;57(03):364–370
5 IPDTOC Working Group. Prevalence at birth of cleft lip with or without cleft palate: data from the International Perinatal Database of Typical Oral Clefts (IPDTOC). Cleft Palate Craniofac J 2011; 48(01):66–81
6 Freitas JA, das Neves LT, de Almeida AL, et al. Rehabilitative treatment of cleft lip and palate: experience of the Hospital for Rehabilitation of Craniofacial Anomalies/USP (HRAC/USP)–Part 1: overall aspects. J Appl Oral Sci 2012;20(01):9–15
7 Trindade IE, Gomes Ade O, Fernandes Mde B, Trindade SH, Silva Filho OG. Nasal airway dimensions of children with repaired unilateral cleft lip and palate. Cleft Palate Craniofac J 2015;52 (05):512–516

8 Trindade-Suedam IK, Lima TF, Campos LD, Yaedú RYF, Filho HN, Trindade IEK. Tomographic pharyngeal dimensions in individuals with unilateral cleft lip/palate and class III malocclusion are reduced when compared with controls. Cleft Palate Craniofac J 2017;54(05):502–508
9 Oosterkamp BC, Remmelink HJ, Pruim GJ, Hoekema A, Dijkstra PU. Craniofacial, craniocervical, and pharyngeal morphology in bilateral cleft lip and palate and obstructive sleep apnea patients. Cleft Palate Craniofac J 2007;44(01):1–7
10 Freitas JA, Garib DG, Trindade-Suedam IK, et al. Rehabilitative treatment of cleft lip and palate: experience of the Hospital for Rehabilitation of Craniofacial Anomalies-USP (HRAC-USP)–part 3: oral and maxillofacial surgery. J Appl Oral Sci 2012;20(06): 673–679
11 Garcia GJ, Tewksbury EW, Wong BA, Kimbell JS. Interindividual variability in nasal filtration as a function of nasal cavity geometry. J Aerosol Med Pulm Drug Deliv 2009;22(02):139–155
12 Mylavarapu G, Murugappan S, Mihaescu M, Kalra M, Khosla S, Gutmark E. Validation of computational fluid dynamics methodology used for human upper airway flow simulations. J Biomech 2009;42(10):1553–1559
13 Lin EL, Bock JM, Zdanski CJ, Kimbell JS, Garcia GJM. Relationship between degree of obstruction and airflow limitation in subglottic stenosis. Laryngoscope 2018;128(07):1551–1557
14 Kimbell JS, Basu S, Garcia GJM, et al. Upper airway reconstruction using long-range optical coherence tomography: Effects of airway curvature on airflow resistance. Lasers Surg Med 2019;51(02): 150–160
15 Faizal WM, Ghazali NNN, Khor CY, et al. Computational fluid dynamics modelling of human upper airway: A review. Comput Methods Programs Biomed 2020;196:105627
16 Cheng T, Carpenter D, Cohen S, Witsell D, Frank-Ito DO. Investigating the effects of laryngotracheal stenosis on upper airway aerodynamics. Laryngoscope 2018;128(04):E141–E149
17 Frank-Ito DO, Wofford M, Schroeter JD, Kimbell JS. Influence of Mesh Density on Airflow and Particle Deposition in Sinonasal Airway Modeling. J Aerosol Med Pulm Drug Deliv 2016;29(01): 46–56
18 Borojeni AAT, Garcia GJM, Moghaddam MG, et al. Normative ranges of nasal airflow variables in healthy adults. Int J CARS 2020;15(01):87–98
19 Campbell DA, Moghaddam MG, Rhee JS, Garcia GJM. Narrowed Posterior Nasal Airway Limits Efficacy of Anterior Septoplasty. Facial Plast Surg Aesthet Med 2021;23(01):13–20
20 Celikoglu M, Buyuk SK, Sekerci AE, Ucar FI, Cantekin K. Three-dimensional evaluation of the pharyngeal airway volumes in patients affected by unilateral cleft lip and palate. Am J Orthod Dentofacial Orthop 2014;145(06):780–786
21 Genta PR, Eckert DJ, Gregorio MG, et al. Critical closing pressure during midazolam-induced sleep. J Appl Physiol 2011;111(05): 1315–1322
22 Ribeiro AA, Smith FJ, Nary Filho H, Trindade IEK, Tonello C, Trindade-Suedam IK. Three-Dimensional Upper Airway Assessment in Treacher Collins Syndrome. Cleft Palate Craniofac J 2020; 57(03):371–377
23 Campos LD, Trindade-Suedam IK, Sampaio-Teixeira AC, et al. Obstructive Sleep Apnea Following Pharyngeal Flap Surgery for Velopharyngeal Insufficiency: A Prospective Polysomnographic and Aerodynamic Study in Middle-Aged Adults. Cleft Palate Craniofac J 2016;53(03):e53–e59
24 Tufik S, Santos-Silva R, Taddei JA, Bittencourt LR. Obstructive sleep apnea syndrome in the Sao Paulo Epidemiologic Sleep Study. Sleep Med 2010;11(05):441–446
25 Alwadei AH, Galang-Boquiren MTS, Kusnoto B, et al. Computerized measurement of the location and value of the minimum sagittal linear dimension of the upper airway on reconstructed lateral cephalograms compared with 3-dimensional values. Am J Orthod Dentofacial Orthop 2018;154(06):780–787
26 Taherian S, Rahai H, Lopez S, Shin J, Jafari B. Evaluation of human obstructive sleep apnea using computational fluid dynamics. Commun Biol 2019;2:423–440
27 Campbell M, Sapra A. Physiology, Airflow Resistance. In: StatPearls. Treasure Island (FL): StatPearls Publishing; April 30, 2021
28 Pfitzner J. Poiseuille and his law. Anaesthesia 1976;31(02):273–275
29 Dempsey JA, Veasey SC, Morgan BJ, O'Donnell CP. Pathophysiology of sleep apnea. Physiol Rev 2010;90(01):47–112
30 Gurani SF, Di Carlo G, Cattaneo PM, Thorn JJ, Pinholt EM. Effect of head and tongue posture on the pharyngeal airway dimensions and morphology in three-dimensional imaging: a systematic review. J Oral Maxillofac Res 2016;7(01):e1
31 Subramaniam RP, Richardson RB, Morgan KT, Kimbell JS, Guilmette RA. Computational fluid dynamics simulations of inspiratory airflow in the human nose and nasopharynx. Inhal Toxicol 1998; 10:91–120
32 Kimbell JS, Garcia GJ, Frank DO, Cannon DE, Pawar SS, Rhee JS. Computed nasal resistance compared with patient-reported symptoms in surgically treated nasal airway passages: a preliminary report. Am J Rhinol Allergy 2012;26(03):e94–e98

